Fermi National Accelerator Laboratory

FERMILAB-Pub-89/206-E
[E-741/CDF]

Two Jet Differential Cross Section in $\bar{p}p$ Collisions at $\sqrt{s}$ = 1.8 TeV*

F. Abe[16] D. Amidei[3], G. Apollinari[11], G. Ascoli[7], M. Atac[4], P. Auchincloss[14], A.R. Baden[6], A. Barbaro-Galtieri[9], V.E. Barnes[12], F. Bedeschi[11], S. Behrends[12], S. Belforte[11], G. Bellettini[11], J. Bellinger[17], J. Bensinger[2], A. Beretvas[14], P. Berge[4], S. Bertolucci[5], S. Bhadra[7], M. Binkley[4], R. Blair[1], C. Blocker[2], J. Bofill[4], A.W. Booth[4], G. Brandenburg[6], D. Brown[6], A. Byon[12], K.L. Byrum[17], M. Campbell[3], R. Carey[6], W. Carithers[9], D. Carlsmith[17], J.T. Carroll[4], R. Cashmore[4], F. Cervelli[11], K. Chadwick[4,12], T. Chapin[13], G. Chiarelli[11], W. Chinowsky[9], S. Cihangir[15], D. Cline[17], D. Connor[10], M. Contreras[2], J. Cooper[4], M. Cordelli[5], M. Curatolo[5], C. Day[4], R. DelFabbro[11], M. Dell'Orso[11], L. DeMortier[2], T. Devlin[14], D. DiBitonto[15], R. Diebold[1], F. Dittus[4], A. DiVirgilio[11], J.E. Elias[4], R. Ely[9], S. Errede[7], B. Esposito[5], A. Feldman[6], B. Flaugher[14], E. Focardi[11], G.W. Foster[4], M. Franklin[6,7], J. Freeman[4], H. Frisch[3], Y. Fukui[8], A.F. Garfinkel[12], P. Giannetti[11], N. Giokaris[13], P. Giromini[5], L. Gladney[10], M. Gold[9], K. Goulianos[13], C. Grosso-Pilcher[3], C. Haber[9], S.R. Hahn[10], R. Handler[17], R.M. Harris[9], J. Hauser[3], Y. Hayashide[16], T. Hessing[15], R. Hollebeek[10], P. Hu[14], B. Hubbard[9], P. Hurst[7], J. Huth[4], H. Jensen[4], R.P. Johnson[4], U. Joshi[14], R.W. Kadel[4], T. Kamon[15], S. Kanda[16], D.A. Kardelis[7], I. Karliner[7], E. Kearns[6], R. Kephart[4], P. Kesten[2], H. Keutelian[7], S. Kim[16], L. Kirsch[2], K. Kondo[16], U. Kruse[7], S.E. Kuhlmann[12], A.T. Laasanen[12], W. Li[1], T. Liss[3], N. Lockyer[10], F. Marchetto[15], R. Markeloff[17], L.A. Markosky[17], P. McIntyre[15], A. Menzione[11], T. Meyer[15], S. Mikamo[8], M. Miller[10], T. Mimashi[16], S. Miscetti[5], M. Mishina[8], S. Miyashita[16], N. Mondal[17], S. Mori[16], Y. Morita[16], A. Mukherjee[4], C. Newman-Holmes[4], L. Nodulman[1], R. Paoletti[11], A. Para[4], J. Patrick[4], T.J. Phillips[6], H. Piekarz[2], R. Plunkett[13], L. Pondrom[17], J. Proudfoot[1], G. Punzi[11], D. Quarrie[4], K. Ragan[10], G. Redlinger[3], J. Rhoades[17], F. Rimondi[4], L. Ristori[11], T. Rohaly[10], A. Roodman[3], A. Sansoni[5], R. Sard[7], V. Scarpine[7], P. Schlabach[7], E.E. Schmidt[4], P. Schoessow[1], M.H. Schub[12], R. Schwitters[6], A. Scribano[11], S. Segler[4], M. Sekiguchi[16], P. Sestini[11], M. Shapiro[6], M. Sheaff[17], M. Shibata[16], M. Shochet[3], J. Siegrist[9], P. Sinervo[10], J. Skarha[17], D.A. Smith[7], F.D. Snider[3], R. St.Denis[6], A. Stefanini[11], Y. Takaiwa[16], K. Takikawa[16], S. Tarem[2], D. Theriot[4], P. Tipton[9], A. Tollestrup[4], G. Tonelli[11], Y. Tsay[3], F. Ukegawa[16], D. Underwood[1], R. Vidal[4], R.G. Wagner[1], R.L. Wagner[4], J. Walsh[10], T. Watts[14], R. Webb[15], T. Westhusing[7], S. White[13], A. Wicklund[1], H.H. Williams[10], T. Yamanouchi[4], A. Yamashita[16], K. Yasuoka[16], G.P. Yeh[4], J. Yoh[4], F. Zetti[11]

[1]*Argonne National Laboratory, Argonne, Illinois 60439* • [2]*Brandeis University, Waltham, Massachusetts 02254* • [3]*University of Chicago, Chicago, Illinois 60637* • [4]*Fermi National Accelerator Laboratory, P.O. Box 500, Batavia, Illinois 60510* • [5]*Laboratori Nazionali di Frascati, Instituto Nazionale do Fisica Nucleare, I-00044, Frascati, Italy* • [6]*Harvard University, Cambridge, Massachusetts 02138* • [7]*University of Illinois, Urbana, Illinois 61801* • [8]*National Laboratory for High Energy Physics (KEK), Tsukuba, Ibaraki 305, Japan* • [9]*Lawrence Berkeley Laboratory, Berkeley, California 94720* • [10]*University of Pennsylvania, Philadelphia, Pennsylvania 19104* • [11]*INFN, University and Sculoa Normale Superiore of Pisa, Pisa, Italy* • [12]*Purdue University, West Lafayette, Indiana 47907* • [13]*Rockefeller University, New York, New York 10021* • [14]*Rutgers University, Piscataway, New Jersey 08854* • [15]*Texas A&M University, College Station, Texas 77843* • [16]*University of Tsukuba, Tsukuba, Ibaraki 305, Japan* • [17]*University of Wisconsin, Madison, Wisconsin 53706*

September 1989

*Submitted to Phys. Rev. Lett.

Two Jet Differential Cross Section in $\bar{p}p$ collisions at $\sqrt{s} = 1.8$ TeV

F. Abe[16], D. Amidei[3], G. Apollinari[11], G. Ascoli[7], M. Atac[4], P. Auchincloss[14], A. R. Baden[6], A. Barbaro-Galtieri[9], V. E. Barnes[12], F. Bedeschi[11], S. Behrends[12], S. Belforte[11], G. Bellettini[11], J. Bellinger[17], J. Bensinger[2], A. Beretvas[14], P. Berge[4], S. Bertolucci[5], S. Bhadra[7], M. Binkley[4], R. Blair[1], C. Blocker[2], J. Bofill[4], A. W. Booth[4], G. Brandenburg[6], D. Brown[6], A. Byon[12], K. L. Byrum[17], M. Campbell[3], R. Carey[6], W. Carithers[9], D. Carlsmith[17], J. T. Carroll[4], R. Cashmore[4], F. Cervelli[11], K. Chadwick[4,12], T. Chapin[13], G. Chiarelli[11], W. Chinowsky[9], S. Cihangir[15] , D. Cline[17], D. Connor[10], M. Contreras[2], J. Cooper[4], M. Cordelli[5], M. Curatolo[5], C. Day[4], R. DelFabbro[11], M. Dell'Orso[11], L. DeMortier[2], T. Devlin[14], D. DiBitonto[15] , R. Diebold[1], F. Dittus[4], A. DiVirgilio[11], J. E. Elias[4], R. Ely[9], S. Errede[7], B. Esposito[5], A. Feldman [6], B. Flaugher[14], E. Focardi[11], G. W. Foster[4], M. Franklin[6,7], J. Freeman[4], H. Frisch[3], Y. Fukui[8], A. F. Garfinkel[12], P. Giannetti [11], N. Giokaris[13], P. Giromini[5], L. Gladney[10], M. Gold[9], K. Goulianos[13], C. Grosso-Pilcher[3], C. Haber[9], S. R. Hahn[10], R. Handler[17], R. M. Harris[9], J. Hauser[3], Y. Hayashide [16], T. Hessing[15] , R. Hollebeek[10], P. Hu[14], B. Hubbard[9], P. Hurst[7], J. Huth[4], H. Jensen[4], R. P. Johnson[4], U. Joshi[14], R. W. Kadel[4], T. Kamon[15] , S. Kanda[16], D. A. Kardelis[7], I. Karliner[7], E. Kearns[6], R. Kephart[4], P. Kesten[2], H. Keutelian[7], S. Kim[16], L. Kirsch[2], K. Kondo[16], U. Kruse[7], S. E. Kuhlmann[12], A. T. Laasanen[12], W. Li[1], T. Liss[3], N. Lockyer[10], F. Marchetto[15] , R. Markeloff[17], L. A. Markosky[17], P. McIntyre[15] , A. Menzione[11], T. Meyer[15] , S. Mikamo[8], M. Miller[10], T. Mimashi[16], S. Miscetti[5], M. Mishina[8], S. Miyashita[16], N. Mondal[17], S. Mori[16], Y. Morita[16], A. Mukherjee[4], C. Newman-Holmes[4], L. Nodulman[1], R. Paoletti[11], A. Para[4], J. Patrick[4], T. J. Phillips[6], H. Piekarz[2], R. Plunkett[13], L. Pondrom[17], J. Proudfoot[1], G. Punzi[11], D. Quarrie[4], K. Ragan[10], G. Redlinger[3], J. Rhoades[17], F. Rimondi[4], L. Ristori[11], T. Rohaly[10], A. Roodman[3], A. Sansoni[5], R. Sard[7], V. Scarpine[7], P. Schlabach[7], E. E. Schmidt[4], P. Schoessow[1], M. H. Schub[12], R. Schwitters[6], A. Scribano[11], S. Segler[4], M. Sekiguchi[16], P. Sestini[11], M. Shapiro[6], M. Sheaff[17], M. Shibata[16], M. Shochet[3], J. Siegrist[9], P. Sinervo[10], J. Skarha[17], D. A. Smith[7], F. D. Snider[3], R. St. Denis[6], A. Stefanini[11], Y. Takaiwa[16],

K. Takikawa[16], S. Tarem[2], D. Theriot[4], P. Tipton[9], A. Tollestrup[4], G. Tonelli[11], Y. Tsay[3], F. Ukegawa[16], D. Underwood[1], R. Vidal[4], R. G. Wagner[1], R. L. Wagner[4], J. Walsh[10], T. Watts[14], R. Webb[15] , T. Westhusing[7], S. White[13], A. Wicklund[1], H. H. Williams[10], T. Yamanouchi[4], A. Yamashita[16], K. Yasuoka[16], G. P. Yeh[4], J. Yoh[4], F. Zetti[11]

[1] Argonne National Laboratory, Argonne, Illinois 60439

[2] Brandeis University, Waltham, Massachusetts 02254

[3] University of Chicago, Chicago, Illinois 60637

[4] Fermi National Accelerator Laboratory, Batavia, Illinois 60510

[5] Laboratori Nazionali di Frascati, Instituto Nazionale di Fisica Nucleare, Frascati, Italy

[6] Harvard University, Cambridge, Massachusetts 02138

[7] University of Illinois, Urbana, Illinois 61801

[8] National Laboratory for High Energy Physics (KEK), Tsukuba, Ibaraki 305, Japan

[9] Lawrence Berkeley Laboratory, Berkeley, California 94720

[10] University of Pennsylvania, Philadelphia, Pennsylvania 19104

[11] INFN, University and Scuola Normale Superiore of Pisa, Italy

[12] Purdue University, West Lafayette, Indiana 47907

[13] Rockefeller University, New York, New York 10021

[14] Rutgers University, Piscataway, New Jersey 08854

[15] Texas A&M University, College Station, Texas 77843

[16] University of Tsukuba, Tsukuba, Ibaraki 305, Japan

[17] University of Wisconsin, Madison, Wisconsin 53706

ABSTRACT

The two jet differential cross section $d^3\sigma(\bar{p}p \rightarrow \text{jet1} + \text{jet2} + \text{X}) \, / dE_t \, d\eta_1 d\eta_2$, averaged over $-0.6 \leq \eta_1 \leq 0.6$, at $\sqrt{s} = 1.8$ TeV, has been measured in the Collider Detector at Fermilab (CDF). The predictions of leading order Quantum Chromodynamics (QCD) for most choices of structure functions show agreement with the data.

The two jet final state, which is dominant at large transverse energies in hadron hadron collisions, has a calculable QCD cross section expressed in terms of the product of point-like scattering cross sections with a pair of structure functions describing the momentum distributions of initial state partons [1]. At leading order the two final state partons are back-to-back in azimuth, and, assuming no initial polarization, have a uniform azimuthal distribution. Three kinematic variables are sufficient to describe the final state in this case. A convenient set, employed here, includes the transverse energy, E_t, common to both partons, together with their pseudorapidities, η_1 and η_2. Pseudorapidity is related to the polar angle , θ, with respect to the proton beam by $\eta = -\ln\tan(\theta/2)$.

Results have been reported previously on measurements of the single jet inclusive E_t spectrum and of the dijet CMS angular distribution [2,3]. Those distributions represent integrals over the other kinematic variables. Good agreement was found between the data and the predictions of leading order QCD calculations. Here we present results of the determination of the double differential cross section, $d^3\sigma/dE_t\,d\eta_1 d\eta_2$ averaged over the interval $-0.6 \leq \eta_1 \leq 0.6$. The double differential cross section is more sensitive to the proton and antiproton structure functions than a single inclusive distribution. The structure functions drop rapidly as the fraction of the proton momenta, x, carried by a parton increases. This results in a dramatic decrease of this cross section at larger values of η_2. As the E_t of the scattered parton increases, this fall-off will occur at successively smaller values of η_2. The low x region and high momentum transfer scale (Q^2) available at the Tevatron allows us to test the validity of the combination of both Quantum Chromodynamics and structure functions in an x region ($0.04 \leq x \leq 0.3$) where gluons are expected to be the dominant initial state partons.

The CDF detector is described elsewhere [4]. This analysis uses information from the vertex time projection chamber, the beam-beam counters, and the electromagnetic and hadronic calorimeters. The calorimeters span the pseudorapidity range $|\eta| < 4.2$. The central calorimeters ($|\eta| < 1.1$) are lead-scintillator sandwiches (electromagnetic) and iron-scintillator sand-

wiches (hadronic), with projective towers segmented in azimuth ($\Delta\phi = 15°$) and pseudorapidity ($\Delta\eta = 0.1$). The plug and forward calorimeters ($1.1 < |\eta| < 4.2$) consist of sandwiches of lead and iron with gas proportional tubes overlaying cathode pads formed into a projective geometry with segmentation in azimuth ($\Delta\phi = 5°$) and pseudorapidity ($\Delta\eta = 0.1$).

In this study, jets are defined by a fixed cone clustering algorithm with a cone radius of $((\Delta\eta)^2 + (\Delta\phi)^2)^{1/2} = 1.0$. The uncorrected energy of a jet is defined as the scalar sum of electromagnetic and hadronic energy in towers associated with the cluster. Transverse energy, E_t, is defined as $E \sin\theta$, where θ is the polar angle of the jet centroid measured at the event vertex. Jet energies are corrected to account for losses due to calorimeter nonlinearities, uninstrumented regions and energy out of the clustering cone; these effects were modeled using an event generator [5] and detector simulation [6]. The corrections of reference [2] were expanded [7] to include an uninstrumented region at $\eta = 0.0$, and to correct for nonuniformities in response as a function of pseudorapidity. The ratio between uncorrected and corrected E_t ranged from $0.80 \pm .07$ for $E_t = 45$ GeV to $0.87 \pm .05$ for $E_t = 225$ GeV where the uncertainties reflect the modeling of detector response to jets and event generation.

Events were recorded with trigger requirements identical to those described in reference [2]. Thresholds on uncorrected tower E_t summed over the central calorimeter were set at 20, 30, 40, and 45 GeV. Offline analysis required at least one central jet ($|\eta| \leq 0.6$) that satisfied the trigger, with a corrected E_t greater than 45, 55, 65 and 75 GeV respectively for each trigger threshold. Simulation studies show that these cuts eliminate fewer than 2% of the events of interest. To ensure that the energy was well contained, the event vertex was required to be within 60 cm of the center of the detector along the beam axis. This reduced the effective integrated luminosities by about 15%. For each trigger threshold the integrated effective luminosity is 0.4 nb^{-1}, 10.5 nb^{-1}, 5.4 nb^{-1} and 5.8 nb^{-1} respectively, with an uncertainty of $\pm$ 15% [8]. The method of reference [2] was employed to reject clusters resulting from beam halo and cosmic ray *bremsstrahlung* . Residual backgrounds ($\leq 1\%$) are negligible for this measurement.

One jet (J1) was required to be within $|\eta_1| \leq 0.6$ and to satisfy the trigger constraint described above. A second jet was required with an uncorrected E_t above 2 GeV. Less than 1% of the triggered events fail this cut. The two leading jets (J1 and J2) in an event are those with the largest uncorrected values of E_t. The second jet was restricted to an interval $|\eta_2| < 2.8$ to avoid large resolution smearing effects (described below). The combination of the above requirements yielded a total of 5291 events. The data were divided into bins of E_t, taken from J1, and η_2, from J2. A raw cross section was derived from the luminosities, the bin widths and the numbers of events in any given bin.

Higher order effects in QCD, such as gluon radiation cause deviations from the ideal $2 \rightarrow 2$ approximation where the values of E_t for the two jets balance and are back-to-back in azimuth. These deviations, along with detector resolution, will affect the measurements of E_t and η_2. We have corrected for these effects using an unsmearing procedure described below. The measured cross section is a convolution of the true cross section with smearing functions in E_t and η_2. These functions were determined by assuming that the momenta of the jets balance in the transverse plane [7,9]. In this plane, two axes are defined, one bisecting the angle between the jets and one perpendicular to this bisector. The momentum imbalance projected onto the bisector is due almost purely to QCD radiation effects [9], whereas the imbalance along the other axis results from a combination of the radiation effects and finite jet resolution. The E_t smearing, including the effects of radiation and detector resolution is well approximated by a Gaussian with an E_t dependent width (σ = 11 GeV for 50 GeV jets, 21 GeV for 150 GeV jets). The η_2 resolution function is taken from the imbalance projected along the bisector, and is approximated by a Lorentzian with an E_t dependent width ($\Gamma = 0.25$ for 50 GeV jets).

To derive the true cross section, $d^3\sigma/dE_t d\eta_1 d\eta_2$ a parameterized function [10] describing the E_t and η_2 spectra was chosen for the $2 \rightarrow 2$ process. A convolution of the input function was formed with the smearing functions in E_t and η_2. The parameters of the input function were varied until the convolved function showed a best fit to the data (χ^2/d.f. = 40/33). Correction

factors were calculated from the ratio of the input function to convolved result. To obtain the true cross section, the raw uncorrected cross section was multiplied by these factors. The values varied from $0.77 \pm .05$ for $|\eta_2| = 0.2$ and $E_t = 150$ GeV to $0.21 \pm .09$ for $|\eta_2| = 2.6$ and $E_t = 60$ GeV.

Table 1 gives the two jet differential cross section. Because the final state is symmetric with respect to the sign of pseudorapidity, the results are expressed in terms of the absolute values of η_2. The systematic uncertainty for each bin includes contributions from the luminosity uncertainty, the resolution corrections, and the jet E_t uncertainty, which is the largest contribution [2]. The cross section is plotted in Fig. 1 for six different bins of E_t, ranging from 45 GeV to 225 GeV and $|\eta_2|$ from 0 to 2.8. The plotted cross section is an average over the range $-0.6 \leq \eta_1 \leq 0.6$. The QCD curves plotted use the EHLQ structure functions (set 2) [11] and take into account different choices for the momentum transfer scale, Q^2, used to evaluate both the strong coupling constant α_s, and to evolve the structure functions. The Q^2 choices in each E_t band correspond to $Q^2 = {E_t}^2/4$, $Q^2 = {E_t}^2$, and $Q^2 = 4{E_t}^2$ for the upper, middle and lower lines respectively. The normalization of the QCD predictions is absolute. The expected falloff in the cross section at higher $|\eta_2|$, caused by the decrease of the structure functions with increasing x, is clearly visible.

To test the sensitivity of our result to differences among commonly used structure functions, a χ^2 was calculated for the predictions of leading order QCD. In all, 12 commonly used sets of structure functions were tested: EHLQ[1], DO[12], DFLM[13] and MRS[14], for the three Q^2 values above. In performing the χ^2 evaluation, the systematic errors were included. The normalizations of the QCD predictions are absolute. The χ^2 test is sensitive to differences among the structure functions in the approximate range $0.05 \leq x \leq 0.3$. Of the 36 possible combinations, 32 had χ^2 values indicating a reasonable fit, where the χ^2 values varied from 23 to 41 for 32 degrees of freedom. Three combinations, DFLM [13] set 3 for $Q^2 = {E_t}^2/4$, DO [12] set 2 for $Q^2 = 4{E_t}^2$, and MRS [14] set 3 for $Q^2 = {E_t}^2/4$ had marginal χ^2 values (47, 50,

and 53 for 32 degrees of freedom). One combination, MRS set 2 for $Q^2 = {E_t}^2/4$, is excluded by our measurement ($\chi^2 = 90$ for 32 DOF); this has a hard gluon distribution with an input parameterization $xG(x) = (1-x)^4(1+9x)$. For this combination, most of the disagreement occurs for data at higher values of x ($x \geq 0.1$).

In summary, the two jet differential cross section in $\bar{p}p$ collisions has been measured and shown to be represented well by leading order QCD calculations made with several combinations of structure function parameterizations and Q^2 scales.

We acknowledge the vital contributions of both the members of the Fermilab accelerator division and the technical staffs of the participating institutions. This work is supported in part by the U.S. Department of Energy and National Science Foundation, the Italian Istituto Nazionale di Fisica Nucleare, the Ministry of Science, Culture and Education of Japan, and the A.P. Sloan Foundation.

References

[1] E. Eichten, I. Hinchliffe, K. Lane and C. Quigg, Rev. of Mod. Phys. **56** (1984) 579.

[2] F. Abe, *et al.*, Phys. Rev. Lett. **62** (1989) 613.

[3] F. Abe, *et al.*, Phys. Rev. Lett. **62** (1989) 3020.

[4] F. Abe *et al.*, Nucl. Instrum. Methods **A271** (1988) 387 and references therein.

[5] F. Paige and S. Protopopescu, in *Proceedings of the Summer Study on the Physics of the Superconducting Supercollider, Snowmass, CO, 1986*, edited by R. Donaldson and J. Marx.

[6] S. Kuhlmann, Ph.D. thesis, Purdue University, 1988 (unpublished); A. Garfinkel (CDF Collaboration), in Proceedings of the Seventh Topical Workshop on Proton Antiproton Collider Physics, edited by R. Raja, A. Tollestrup and J. Yoh, World Scientific, Singapore (1989).

[7] R. M. Harris, Ph.D. thesis, U. C. Berkeley, LBL-27246 (1989).

[8] F. Abe *et al.*Phys. Rev. Lett. **61**(1988) 1819.

[9] The method used was an extension of the technique outlined in P. Bagnaia *et al.*, Phys. Lett. **144B** (1984) 283.

[10] The single effective subprocess approximation is employed, as described by B. Combridge and C. Maxwell, Nucl. Phys. **B239** (1984) 429, with the $qg \rightarrow qg$ angular distribution as the effective angular distribution. The proton effective structure function is parameterized by $F(x) = A(1-x)^{P1}/x^{P2}$, where A is an amplitude and $P1$ and $P2$ are the two parameters varied in the fit.

[11] The structure functions described in ref. 1, sets 1 and 2.

[12] D. W. Duke and J. F. Owens, Phys. Rev. **D30** (1984) 49 (sets 1 and 2).

[13] M. Diemoz, F. Ferroni, E. Longo, and G. Martinelli, Z. Phys. **C39** (1988) 21 (sets 1,2 and 3).

[14] A. D. Martin, R. G. Roberts, and W. J. Stirling, Phys. Rev.**D37** (1988) 1161 (sets 1,2 and 3) and MRS set BCDMS and set EMC in Phys. Lett. **B206** (1988) 327.

FIG. 1. The two jet differential cross section, for $|\eta_1| < 0.6$, compared to a range of QCD predictions described in the text. The inner error bars are statistical, and the outer error bars include the statistical error and the E_t and η_2 dependent part of the systematic error. A normalization uncertainty (E_t and η_2 independent part) of +41% and −30%, common to all points, is also indicated.

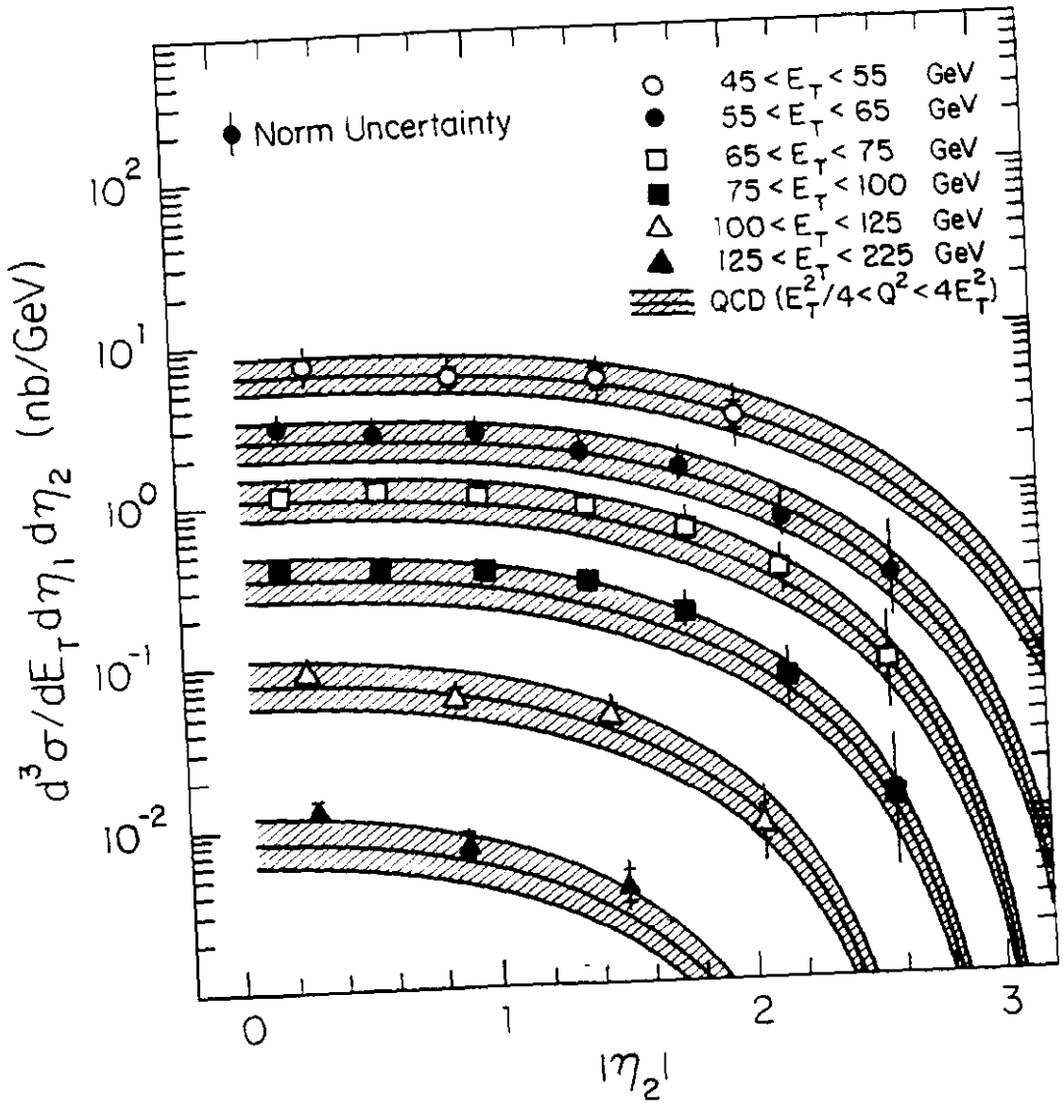

TABLE 1. The two jet differential cross section at $\sqrt{s} = 1.8$ TeV. The systematic error quoted includes all known systematic uncertainties, including the effect of uncertainties in the energy scale. The cross section is an average over the range $-0.6 \leq \eta_1 \leq 0.6$.

E_t Range (GeV)	$\langle E_t \rangle$ (GeV)	$\lvert\eta_2\rvert$ Range	$\langle \lvert\eta_2\rvert \rangle$	$d^3\sigma/dE_t d\eta_1 d\eta_2$ (nb/GeV)	Stat. Err. (%)	Sys. Err. (%)
45–55	49.6	0.0–0.6	0.32	7.24	±13	+ 52/ − 36
45–55	49.7	0.6–1.2	0.90	5.86	±14	+ 52/ − 36
45–55	49.2	1.2–1.8	1.47	5.30	±14	+ 53/ − 36
45–55	49.3	1.8–2.4	2.00	2.97	±18	+ 62/ − 41
55–65	59.4	0.0–0.4	0.21	3.08	± 4	+ 45/ − 33
55–65	59.3	0.4–0.8	0.59	2.82	± 5	+ 46/ − 33
55–65	59.1	0.8–1.2	0.99	2.72	± 5	+ 46/ − 33
55–65	59.7	1.2–1.6	1.39	2.01	± 5	+ 47/ − 34
55–65	59.2	1.6–2.0	1.78	1.52	± 6	+ 51/ − 36
55–65	59.5	2.0–2.4	2.17	0.714	± 8	+ 61/ − 39
55–65	59.2	2.4–2.8	2.60	0.306	±10	+103/ − 55
65–75	69.6	0.0–0.4	0.20	1.22	± 6	+ 42/ − 31
65–75	69.2	0.4–0.8	0.60	1.23	± 6	+ 42/ − 31
65–75	69.4	0.8–1.2	0.99	1.05	± 6	+ 43/ − 32
65–75	69.6	1.2–1.6	1.41	0.889	± 7	+ 44/ − 32
65–75	69.1	1.6–2.0	1.80	0.656	± 7	+ 49/ − 35
65–75	69.4	2.0–2.4	2.16	0.319	±10	+ 60/ − 40
65–75	68.7	2.4–2.8	2.57	0.0866	±15	+106/ − 57
75–100	84.6	0.0–0.4	0.19	0.411	± 6	+ 42/ − 31
75–100	84.0	0.4–0.8	0.60	0.395	± 6	+ 43/ − 32
75–100	84.1	0.8–1.2	1.00	0.365	± 6	+ 43/ − 32
75–100	83.8	1.2–1.6	1.40	0.302	± 6	+ 44/ − 32
75–100	83.0	1.6–2.0	1.78	0.189	± 8	+ 50/ − 36
75–100	83.2	2.0–2.4	2.17	0.0707	±11	+ 65/ − 43
75–100	81.0	2.4–2.8	2.58	0.0132	±17	+132/ − 69
100–125	109.2	0.0–0.6	0.28	0.0952	±10	+ 42/ − 32
100–125	109.6	0.6–1.2	0.87	0.0616	±12	+ 43/ − 32
100–125	112.5	1.2–1.8	1.47	0.0458	±13	+ 47/ − 34
100–125	108.2	1.8–2.4	2.05	0.00925	±24	+ 70/ − 48
125–225	149.1	0.0–0.6	0.30	0.0130	±14	+ 41/ − 30
125–225	148.4	0.6–1.2	0.90	0.00765	±17	+ 42/ − 31
125–225	145.6	1.2–1.8	1.51	0.00404	±22	+ 53/ − 37

Table 1. Two Jet Differential Cross Section Values and Uncertainties